

TR/13/86

September 1986

Mean drift forces on arrays of bodies  
due to incident long waves

by

P. McIver

z 1469503

Abstract

The scattering of long water waves by an array of bodies is investigated using the method of matched asymptotic expansions. Two particular geometries are considered, these are a group of vertical cylinders extending throughout the depth and a group of floating hemispheres. From these solutions, the low-frequency limit of the ratio of the mean drift force on a group of  $N$  bodies to that on a single body is calculated. For a wide range of circumstances this drift force ratio is  $N^2$  which is in agreement with previous numerical work. Further drift force enhancement is possible for certain configurations of vertical cylinders.



## 1. Introduction

Bodies floating in irregular seas may experience low-frequency oscillations as a result of second-order interactions between different frequency components of the incident wave train. Newman (1974) has shown that the slowly-varying forces that give rise to these oscillations may be related to the mean drift forces on the body in monochromatic waves at a frequency corresponding to that of the oscillations. The mean drift force is easier to model than the slowly-varying force, though also a second-order effect it depends only on the first-order solution. Thus, if the linear scattering problem can be solved the mean drift force may be calculated. For further information on second-order wave forces, see, for example, Pinkster (1979).

Recent numerical results of Eatock-Taylor and Hung (1985) concerning mean drift forces on multi-column structures have shown that interaction effects between structural elements may be very important at low frequencies. Their work suggests that for certain geometries the mean horizontal drift force on a group of  $N$  bodies may be of the order of  $N^2$  times the forces on a single body when the incident waves are long compared to the overall body size. In a discussion accompanying that paper the present author indicated briefly how this ' $N^2$  law' may be verified analytically for an array of widely-spaced cylinders. In the present work a more rigorous and extensive investigation of this behaviour is undertaken. In particular, the long-wave limit of the mean, drift force is calculated for an array of vertical cylinders extending throughout the water depth and for an array of hemispheres floating on water of infinite depth. In the former case the  $N^2$  law does not always hold, for closely-spaced bodies there may be additional enhancement effects, but for an array of hemispheres the law is exact in the low-frequency limit. Consideration of a known solution for scattering by a single truncated cylinder suggests that any additional enhancement, as exhibited in the vertical cylinder case, will be small for most floating bodies.

As stated above, the mean drift force is calculated from the solution of the linear diffraction problem. A number of authors have proposed solution procedures for wave scattering by an array of arbitrary bodies that can, in principle, be used for all wave frequencies and body spacings, for example that due to Kagemoto and Yue (1985). However, none of these methods can yield, easily, analytical results for the long-wave limit. In the present work the problem of the scattering of long waves by an array of bodies is solved using the method of matched asymptotic expansions. The basic procedure is similar to that used by Balsa (1977, 1982 and 1983) for work in acoustics on low-frequency flow through an array of bodies, consequently some details of the matching will not be given here.

The horizontal mean drift force may be calculated from the linear diffraction potential in two ways, either by direct integration of a quadratic term over the body surface or indirectly from the far-field potential. Here the latter procedure, due to Maruo (1960), is employed so the leading-order approximation to the far-field potential for long waves is required. The general formulation of the scattering problem is given in section 2 while the solutions for an array of cylinders and an array of hemispheres are described in sections 3 and 4 respectively. Finally, in section 5, expressions for the mean drift force are presented and discussed.

## 2. General formulation

A plane wave-train of amplitude  $A$  and frequency  $\omega$  is incident upon an array of  $N$  fixed bodies in water of constant depth  $h$ . Cartesian coordinates  $(x,y,z)$  are defined so that the  $(x,y)$ -plane corresponds to the mean free surface and the  $z$ -axis is directed vertically downwards. The origin of coordinates is chosen to be within the array. It will also be convenient to employ cylindrical polar coordinates  $(r,\psi,z)$  and spherical polar coordinates  $(p,\theta,\psi)$ , defined as shown in Figure 1. Coordinate systems with origin at the centre of the waterplane area of each body will also be used, a subscript  $j$  will indicate coordinates associated with body  $j$ . The origin of coordinate system  $j$  is at  $(x,y,z) = (\xi_j, \eta_j, 0)$ , while the position of body  $\ell$  relative to body  $j$  has polar coordinates  $(r_j, \psi_j) = (R_{j\ell}, \alpha_{j\ell})$ . A plan view of the array is given in Figure 2.

The usual assumptions of the linearised theory of water waves are made, including those of inviscid, irrotational flow. Hence the fluid motion is described by a velocity potential

$$\Phi_T(x,y,z,t) = \text{Re} \left\{ -\frac{igA}{\omega} \phi_T(x,y,z) e^{i\omega t} \right\} \quad (2.1)$$

where  $g$  is the acceleration due to gravity. The complex-valued function  $\phi_T(x,y,z)$  satisfies

$$\nabla^2 \phi_T = 0 \quad (2.2)$$

within the fluid, the linearised free surface condition

$$\frac{\partial \phi_T}{\partial z} + \frac{\omega^2}{g} \phi_T = 0, \quad z=0 \quad (2.3)$$

(excluding the waterplane area of each body) and zero-flux conditions on the bed  $z = h$  and the wetted surface of each body. The scattered part of the wave field must also satisfy a radiation condition allowing only outward propagating waves at large horizontal distances from the array.

The scattering problem is solved by the method of matched asymptotic expansions under the assumptions that  $\mu = k\ell \ll 1$  and  $\epsilon = a/\ell \ll 1$  (which together

imply  $\mu\epsilon = ka \ll 1$ ). Here  $k$  is the wavenumber, related to the radian frequency  $\omega$  through the dispersion relation

$$\omega^2 = gk \tanh kh, \quad (2.4)$$

$\ell$  is a typical body spacing and  $a$  is a typical body radius. The first of the assumptions above indicates that the waves are long relative to the horizontal extent of the array (thus the array must be of finite horizontal extent) while the second requires the bodies to be widely-spaced relative to body-size, though interaction effects beyond the lowest order in  $\epsilon$  will be included in the following analysis.

Following Balsa (1982,1983), three flow regions are distinguished. These are: an outer region at large distances from the array where the length scale is  $k^{-1}$ , an intermediate region within the array (but not 'close' to any body) where the length scale is  $\ell$  and  $N$  inner regions surrounding each body where the length scale is  $a$ . In the outer region the scattered wave appears to be the result of singularities at a single origin whilst in the intermediate region the disturbance appears to be generated by singularities at the origin of each body coordinate system.

The previous work of Balsa makes it unnecessary to give full details of the solution derivation here. In particular the correct gauge functions for the various asymptotic expansions will be assumed from the outset. For each of the two body geometries considered the solution is presented in the following way. The potentials in each of the three regions are expanded in terms of gauge functions in  $\mu$  and the outer and intermediate expansions matched so that the leading order outer solution is determined in terms of constants in the intermediate solution. The potentials in the intermediate and inner regions are further expanded in terms of gauge functions in  $\epsilon$ . The body boundary conditions are satisfied in the inner regions and matching determines the intermediate solution and hence the outer solution. The final form of the far field potential is a double expansion in  $\mu$  and  $\epsilon$ .

### 3. An array of vertical cylinders

Each body is taken to be a vertical circular cylinder of radius  $a$ , extending throughout the depth of the fluid. The incident wave travels in the direction of increasing  $x$  so that  $\phi_T$  may be written

$$\phi_T(x,y,z) = \left\{ e^{ikx} + \phi(x,y) \right\} \frac{\cosh k(z-h)}{\cosh kh} \quad (3.1)$$

where the first term within the braces represents the incident wave and  $\phi$  the scattered wave. Substitution of this expression for  $\phi_T$  into equation (2.2) gives

$$\frac{\partial^2 \phi}{\partial x^2} + \frac{\partial^2 \phi}{\partial y^2} + k^2 \phi = 0. \quad (3.2)$$

The free surface condition (2.3) and the zero flux condition on  $z = h$  are satisfied identically because of the special choice of form of  $\phi_T$ . The function

$\phi$  must satisfy the boundary conditions

$$\frac{\partial \phi}{\partial r_j} = -\frac{\partial}{\partial r_j} (e^{ikx}), \quad r_j = a \quad (j=1,2,\dots,N) \quad (3.3)$$

on the wetted surfaces of the cylinders.

### 3.1 Outer/intermediate matching

Scaled coordinates for the outer region are defined by

$$\hat{x} = kx, \hat{y} = ky, \hat{r} = kr \quad (3.4)$$

so that, from equation (3.2),  $\hat{\phi}(\hat{x}, \hat{y})$  ( $\equiv \phi(x, y)$ ) satisfies

$$\frac{\partial^2 \hat{\phi}}{\partial \hat{x}^2} + \frac{\partial^2 \hat{\phi}}{\partial \hat{y}^2} + \hat{\phi} = 0 \quad (3.5)$$

in the fluid region. In the intermediate region appropriate scaled coordinates are defined by

$$\bar{x} = x/\ell, \bar{y} = y/\ell, \bar{r} = r/\ell \quad (3.6)$$

and  $\bar{\phi}(\bar{x}, \bar{y})$  ( $\equiv \phi(x, y)$ ) satisfies

$$\frac{\partial^2 \bar{\phi}}{\partial \bar{x}^2} + \frac{\partial^2 \bar{\phi}}{\partial \bar{y}^2} + \mu^2 \bar{\phi} = 0 \quad (3.7)$$

within the fluid. The outer and intermediate potentials are expanded in  $\mu$  as

$$\hat{\phi} = \mu^2 \hat{\phi}^{(2)} + O(\mu^3) \quad (3.8)$$

and

$$\bar{\phi} = \mu \bar{\phi}^{(1)} + \mu^2 \ell n \mu \bar{\phi}^{(2.1)} + \mu^2 \bar{\phi}^{(2)} + O(\mu^3) \quad (3.9)$$

respectively, here only those terms required to determine the outer potential to leading order are displayed explicitly. In the current work the order symbol  $O(\mu^S)$  is used to denote terms of order  $y \mu^S (\ell n \mu)^t$  for all  $t$  greater than or equal to zero. A superscript within parentheses identifies individual terms within an expansion.

The most general solution for  $\hat{\phi}^{(2)}$  satisfying equation (3.5) and the radiation condition is

$$\hat{\phi}^{(2)} = \hat{A}_0 H_0(\hat{r}) + \sum_{m=1}^{\infty} \left( \hat{A}_m \cos m\psi + \hat{B}_m \sin m\psi \right) H_m(\hat{r}) \quad (3.10)$$



where  $H_m$  denotes the Hankel function of the first kind and order  $m$  and

$\hat{A}_0^{(2)}, \hat{A}_1^{(2)}, \dots, \hat{B}_1^{(2)}, \dots$  are complex constants to be determined from the matching. Substitution of equation (3.9) into equation (3.7) shows that each term in the expansion of  $\bar{\phi}$ , to the order displayed, is a solution of the two-dimensional Laplace equation. The most convenient form for each  $\bar{\phi}^{(t)}$  ( $t = 1, 2, 1, 2$ ) is in terms of singularities within each body, thus

$$\bar{\phi}^{(t)} = \bar{A}^{(t)} + \sum_{j=1}^N \left\{ \bar{B}_{j0}^{(t)} \ell_n \bar{r}_j + \sum_{m=1}^{\infty} \left( \bar{A}_{jm}^{(t)} \cos m\psi_j + \bar{B}_{jm}^{(t)} \sin m\psi_j \right) \bar{r}_j^{-m} \right\} \quad (3.11)$$

where  $\bar{A}_0^{(t)}, \bar{A}_{j_1}^{(t)}, \dots, \bar{B}_{j_0}^{(t)}, \dots$  are complex constants to be determined. The expansions to  $O(\mu^2)$  of  $\hat{\phi}$  and  $\bar{\phi}$  may now be matched following the principles described by Van Dyke (1975). As a result the outer solution may be written in terms of the constants in the intermediate solution as

$$\hat{\phi}^{(2)} = \frac{\bar{A}_0^{(2)}}{\Gamma} H_0(\hat{r}) + \frac{\pi i}{2} \sum_{j=1}^N \left( \bar{A}_{j1}^{(1)} \cos \psi + \bar{B}_{j1}^{(1)} \sin \psi \right) H_1(\hat{r}) \quad (3.12)$$

where

$$\Gamma = 1 + \frac{2i}{\pi} (\gamma - \ell_n 2) \quad (3.13)$$

and  $\gamma = 0.577215\dots$  is Euler's constant. Most of the constants in the intermediate solution are still undetermined though the following relations are noted:

$$\bar{A}_0^{(1)} = 0; \bar{B}_{j_0}^{(1)} = 0, j = 1, 2, \dots, N \quad (3.14)$$

$$\bar{A}_0^{(2,1)} = \frac{2i}{\pi \Gamma} \bar{A}_0^{(2)} = \sum_{j=1}^N \bar{B}_{j_0}^{(2)}.$$

### 3.2 Intermediate/inner matching

The scaled coordinates for the inner region of body  $j$  are defined by

$$\tilde{x}_j = (x - \xi_j)/a, \tilde{y}_j = (y - \eta_j)/a, \tilde{r}_j = (\tilde{x}_j^2 + \tilde{y}_j^2)^{\frac{1}{2}} \quad (3.15)$$

so that, from equation (3.2),  $\tilde{\phi}_j(\tilde{x}_j, \tilde{y}_j) (\equiv \phi(x, y))$  satisfies

$$\frac{\partial^2 \tilde{\phi}_j}{\partial \tilde{x}_j^2} + \frac{\partial^2 \tilde{\phi}_j}{\partial \tilde{y}_j^2} + (\mu \epsilon)^2 \tilde{\phi}_j = 0. \quad (3.16)$$

The body boundary condition (3.3) becomes

$$\frac{\partial \tilde{\phi}_j}{\partial \tilde{r}_j} = - \frac{\partial}{\partial \tilde{r}_j} \{ \exp (i\mu (\epsilon \tilde{x}_j + \bar{\xi}_j)) \}, \tilde{r}_j = 1 \quad (3.17)$$

where  $\bar{\xi}_j = \bar{\xi}_j / \ell$ .

As for the intermediate solution (equation (3.9)), the inner solution is posed first as an expansion in  $\mu$  of the form

$$\tilde{\phi}_j = \mu \tilde{\phi}_j^{(1)} + \mu^2 \ell n \mu \tilde{\phi}_j^{(2,1)} + \mu^2 \tilde{\phi}_j^{(2)} + O(\mu^3) \quad (3.18)$$

where each term displayed is a solution of Laplace's equation. The individual terms of the expansions in  $\mu$  for  $\bar{\phi}$  and  $\tilde{\phi}_j$  are now expanded in  $\epsilon$ . Beginning with the first non-zero term, the expansions for the inner potential are

$$\tilde{\phi}_j^{(1)} = \epsilon \tilde{\phi}_j^{(1,1)} + \epsilon^2 \tilde{\phi}_j^{(1,2)} + \dots \quad (3.19)$$

and

$$\tilde{\phi}_j^{(2)} = \epsilon \tilde{\phi}_j^{(2,1)} + \epsilon^2 \ell n \epsilon \tilde{\phi}_j^{(2,2,1)} + \epsilon^2 \tilde{\phi}_j^{(2,2)} + \dots \quad (3.20)$$

The appearance of the  $\epsilon^2 \ell n \epsilon$  term in equation (3.20) is due to a source-like term in  $\tilde{\phi}_j^{(2,2)}$ , all other gauge functions are powers of  $\epsilon$ . Similar expansions

are adopted for the intermediate solution though these contain only integer powers of  $\epsilon$ , beginning with  $\epsilon^2$ . The expansion of the intermediate solution in  $\epsilon$  is equivalent to expanding the constant coefficients in equation (3.11) and this interpretation will be used here. An expansion for  $\tilde{\phi}_j^{(2,1)}$  is not given

above as it is particularly simple, it turns out that only constant terms may be matched with the intermediate solution. The corresponding term in the intermediate expansion reduces to the same constant so that

$$\tilde{\phi}_j^{(2,1)} = \bar{\phi}^{(2,1)} = \bar{A}_0^{(2,1)} \quad (3.21)$$

which, by equation (3.14), is determined by  $\bar{A}_0^{(2)}$ .

The body boundary conditions for  $\tilde{\phi}_j^{(1,1)}$ ,  $\tilde{\phi}_j^{(2,1)}$  and  $\tilde{\phi}_j^{(2,2)}$  are, from equation (3.17),

$$\frac{\partial \tilde{\phi}_j^{(1,1)}}{\partial \tilde{r}_j} = -i \cos \psi_j, \tilde{r}_j = 1, \quad (3.22)$$

$$\frac{\partial \tilde{\phi}_j^{(2,1)}}{\partial \tilde{r}_j} = \bar{\xi}_j \cos \psi_j, \tilde{r}_j = 1, \quad (3.23)$$

and

$$\frac{\partial \tilde{\phi}_j^{(2,2)}}{\partial \tilde{r}_j} = \cos^2 \psi_j, \tilde{r}_j = 1. \quad (3.24)$$

All other terms on the right-hand side of equations (3.19) and (3.20) must satisfy the condition of zero normal derivative on the body surfaces. The general form of  $\tilde{\phi}_j^{(s,t)}$  which satisfies Laplace's equation and has zero normal derivative on body  $j$  is

$$\tilde{\phi}_{j,c}^{(s,t)} = \tilde{A}_{j0}^{(s,t)} + \sum_{m=1}^{\infty} \left( \tilde{A}_{jm}^{(s,t)} \cos m\psi_j + \tilde{B}_{jm}^{(s,t)} \sin m\psi_j \right) \left( \tilde{r}_j^m + \tilde{r}_j^{-m} \right) \quad (3.25)$$

For  $\tilde{\phi}_j^{(1,1)}$ ,  $\tilde{\phi}_j^{(2,1)}$  and  $\tilde{\phi}_j^{(2,2)}$  particular solutions satisfying the boundary conditions (3.22-24) are to be added to this; these are

$$\tilde{\phi}_{j,p}^{(1,1)} = i \frac{\cos \psi_j}{\tilde{r}_j} \quad (3.26)$$

$$\tilde{\phi}_{j,p}^{(2,1)} = -\bar{\xi}_j \frac{\cos \psi_j}{\tilde{r}_j} \quad (3.27)$$

and

$$\tilde{\phi}_{j,p}^{(2,2)} = \frac{1}{2} \ln \tilde{r}_j - \frac{1}{2} \frac{\cos 2\psi_j}{\tilde{r}_j^2} \quad (3.28)$$

Matching these forms of the inner solution with the intermediate solution (3.11) yields

$$\begin{aligned} \bar{A}_{j\ell}^{(1)} &= \epsilon^2 i \left\{ 1 - \epsilon^2 \sum_{\substack{p=1 \\ p \neq n}}^N \frac{\cos 2\alpha_{np}}{\bar{R}_{np}^2} \right\} \\ \bar{B}_{j\ell}^{(1)} &= -\epsilon^4 i \sum_{\substack{p=1 \\ p \neq n}}^N \frac{\sin 2\alpha_{np}}{\bar{R}_{np}^2} \\ \bar{A}_0^{(2)} &= \epsilon^2 \frac{\pi \Gamma N}{4 i} \end{aligned} \quad (3.29)$$

correct to order  $\epsilon^4$ . A careful examination of the matching equations shows the expression for  $\bar{A}_0^{(2)}$  to be exact. The coefficients in equations (3.29) determine the outer solution to leading order in  $\mu$ . Details of the inner and intermediate solutions are not required in the present work, though for completeness they are recorded in the Appendix.

#### 4. An array of floating hemispheres

Let each body be a floating hemisphere (i.e. with the plane face at the mean free surface) of radius  $a$ . The water depth is taken to be infinite, that is  $kh \rightarrow \infty$  in equation (2.4), so that a wave train incident from large negative  $x$  is described by the potential

$$\phi_{\text{inc}} = \exp \{K(ix - z)\} \quad (4.1)$$

where the wavenumber  $K = \omega^2/g$ . The scattered wave potential  $\phi(x, y, z)$  must satisfy equations (2.2) and (2.3) with the body boundary conditions

$$\frac{\partial \phi}{\partial \rho_j} = - \frac{\partial}{\partial \rho_j} e^{K(ix-z)}, \quad \rho_j = a \quad (j=1,2,\dots,N), \quad (4.2)$$

where  $\rho_j$  is a spherical polar coordinate as defined in section 2.

##### 4.1 Outer/intermediate matching

Scaled coordinates for the outer region are defined by

$$\hat{x} = KX, \quad \hat{y} = Ky, \quad \hat{z} = Kz \quad (4.3)$$

so that  $\hat{\phi}(\hat{x}, \hat{y}, \hat{z}) (\equiv \phi(x, y, z))$  satisfies Laplace's equation within the fluid region and the free surface condition

$$\frac{\partial \hat{\phi}}{\partial \hat{z}} + \hat{\phi} = 0, \quad \hat{z} = 0 \quad (4.4)$$

For the intermediate region appropriate scaled coordinates are

$$\bar{x} = x/\ell, \quad \bar{y} = y/\ell, \quad \bar{z} = z/\ell \quad (4.5)$$

so that  $\bar{\phi}(\bar{x}, \bar{y}, \bar{z}) (\equiv \phi(x, y, z))$  satisfies Laplace's equation in the fluid region and the free surface condition

$$\frac{\partial \bar{\phi}}{\partial \bar{z}} + \mu \bar{\phi} = 0, \quad \bar{z} = 0 \quad (4.6)$$

where  $\mu = K\ell$ . In contrast to the vertical cylinder case, the leading order outer solution is fully determined by the leading order intermediate solution; put

$$\hat{\phi} = \mu^2 \hat{\phi}^{(2)} + O(\mu^3) \quad (4.7)$$

and

$$\bar{\phi} = \mu \bar{\phi}^{(1)} + O(\mu^2) \quad (4.8)$$

The outer solution  $\hat{\phi}^{(2)}$  may be expressed in terms of generalised wave sources (Thorne (1953)) so that

$$\hat{\phi}^{(2)} = \hat{A}_0 \psi_0(\hat{r}) + \sum_{m=1}^{\infty} \left( \hat{A}_m \cos m\psi + \hat{B}_m \sin m\psi \right) \psi_m(\hat{r}) \quad (4.9)$$

where

$$\psi_m(\hat{r}) = \int_0^\infty \frac{k^{m+1}}{k-1} e^{-k\hat{z}} J_m(k\hat{r}) dk \quad (4.10)$$

and  $J_m$  is a Bessel function of the first kind and order  $m$ . Each source individually satisfies Laplace's equation, the free surface condition (4.4) and the radiation condition. The intermediate solution  $\bar{\phi}^{(1)}$  is constructed from singularities within each body that satisfy Laplace's equation and, from equations (4.6) and (4.8),

$$\frac{\partial \bar{\phi}^{(1)}}{\partial \theta_j} = 0, \quad \theta_j = \pi/2 \quad (4.11)$$

thus

$$\begin{aligned} \bar{\phi}^{(1)} = & \sum_{j=1}^N \left\{ \sum_{n=0}^{\infty} \bar{A}_{j,0n}^{(1)} \frac{P_{2n}(\cos \theta_j)}{\bar{\rho}_j^{2n+1}} \right. \\ & + \sum_{m=1}^{\infty} \sum_{n=m}^{\infty} \left( \bar{A}_{j,mn}^{(1)} \cos 2m\psi_j + \bar{B}_{j,mn}^{(1)} \sin 2m\psi_j \right) \frac{p_{2n}^{2m}(\cos \theta_j)}{\bar{\rho}^{2n+1}} \\ & \left. + \sum_{m=0}^{\infty} \sum_{n=m}^{\infty} \left( \bar{C}_{j,mn}^{(1)} \cos (2m+1)\psi_j + \bar{D}_{j,mn}^{(1)} \sin (2m+1)\psi_j \right) \frac{p_{2n+1}^{2m+1}(\cos \theta_j)}{\bar{\rho}^{2n+2}} \right\} \quad (4.12) \end{aligned}$$

where  $P_n^m$  is the associated Legendre function of degree  $n$  and order  $m$  (note that (4.11) is satisfied by taking  $m+n$  to be even). The complex constants  $\hat{A}_0^{(2)}, \hat{A}_1^{(2)}, \dots, \hat{B}_1^{(2)}, \dots$  and  $\hat{A}_{j,00}^{(1)}, \dots$  are determined by the matching. The expansion of  $\psi_m$  in spherical polar coordinates, required for the matching, is given by Hulme (1982), along with a number of other results relevant to the present work. The leading order outer solution is

$$\hat{\phi}^{(2)} = \psi_0(\hat{r}) \sum_{j=1}^N \bar{A}_{j,00} \quad (4.13)$$

which depends only on the magnitude of the apparent source within each body.

## 4.2 Intermediate/inner matching

The scaled coordinates for the inner region of body  $j$  are defined by

$$\tilde{x}_j = (x - \xi_j)/a, \quad \tilde{y}_j = (y - \eta_j)/a, \quad \tilde{z} = z/a, \quad \tilde{\rho}_j = (x_j^2 + y_j^2 + z_j^2)^{\frac{1}{2}} \quad (4.14)$$

so that  $\tilde{\phi}_j(\tilde{x}_j, \tilde{y}_j, \tilde{z}_j) (\equiv \phi(x, y, z))$  satisfies Laplace's equation, the free surface condition

$$\frac{\partial \tilde{\phi}_j}{\partial \tilde{z}} + \mu \in \tilde{\phi}_j = 0, \tilde{z} = 0 \quad (4.15)$$

and the body boundary condition

$$\frac{\partial \tilde{\phi}_j}{\partial \tilde{\rho}_j} = -\frac{\partial}{\partial \tilde{\rho}_j} \{ \exp(\mu(\in i\tilde{x}_j + i\tilde{\xi}_j - \in \tilde{z})) \}, \tilde{\rho}_j = 1. \quad (4.16)$$

The inner solution is expanded in  $\mu$  as

$$\tilde{\phi}_j = \mu \tilde{\phi}_j^{(1)} + O(\mu^2) \quad (4.17)$$

and then  $\tilde{\phi}_j^{(1)}$  is further expanded in  $\in$  as

$$\tilde{\phi}_j^{(1)} = \in \tilde{\phi}_j^{(1,1)} + \in^2 \tilde{\phi}_j^{(1,2)} + \dots, \quad (4.18)$$

all the gauge functions being integer powers of  $\in$ . A similar expansion is adopted for  $\bar{\phi}^{(1)}$  though, as previously, it is perhaps simpler to think of it as an expansion of the coefficients in equation (4.12).

The body boundary condition for  $\tilde{\phi}_j^{(1,1)}$  is, from equation (4.16),

$$\frac{\partial \tilde{\phi}_j^{(1,1)}}{\partial \tilde{\rho}_j} = -(i \sin \theta_j \cos \psi_j - \cos \theta_j), \tilde{\rho}_j = 1 \quad (4.19)$$

while the remaining terms on the right-hand side of equation (4.18) have zero normal derivative on the body surface. The free surface condition (4.15) yields

$$\frac{\partial \tilde{\phi}_j^{(1,t)}}{\partial \theta_j} = 0, \theta_j = \pi/2 \quad (t=1,2,\dots). \quad (4.20)$$

The general solution of Laplace's equation satisfying equation (4.20) and having zero normal derivative on  $\tilde{\rho}_j = 1$

$$\begin{aligned} \tilde{\phi}_{j,c}^{(1,t)} &= \sum_{n=0}^{\infty} \tilde{A}_{j,0n}^{(1,t)} \left( \tilde{\rho}_j^{2n} + \frac{2n}{(2n+1)\tilde{\rho}_j^{2n+1}} \right) P_{2n}(\cos \theta_j) \\ &+ \sum_{m=1}^{\infty} \sum_{n=m}^{\infty} \left( \tilde{A}_{j,mn}^{(1,t)} \cos 2m\psi_j + \tilde{B}_{j,mn}^{(1,t)} \sin 2m\psi_j \right) \left( \tilde{\rho}_j^{2n} + \frac{2n}{(2n+1)\tilde{\rho}_j^{2n+1}} \right) P_{2n}^{2m}(\cos \theta_j) \\ &+ \sum_{m=0}^{\infty} \sum_{n=m}^{\infty} \left( \tilde{C}_{j,mn}^{(1,t)} \cos (2m+1)\psi_j + \tilde{D}_{j,mn}^{(1,t)} \sin (2m+1)\psi_j \right) \left( \tilde{\rho}_j^{2n+1} + \frac{2n+1}{(2n+2)\tilde{\rho}_j^{2n+2}} \right) P_{2n+1}^{2m+1}(\cos \theta_j) \end{aligned} \quad (4.21)$$

with the complex constants  $\tilde{A}_{j,00}^{(1,t)}, \dots$  to be determined from the matching. For

$\tilde{\phi}_j^{(1,1)}$  there is an additional particular solution, satisfying equation (4.19),

$$\tilde{\phi}_j^{(1,1)} = \frac{i \sin \theta_j \cos \psi_j}{2\tilde{\rho}_j^2} - \sum_{n=0}^{\infty} \frac{E_n P_{2n}(\cos \theta_j)}{(2n+1) \tilde{\rho}_j^{2n+1}}$$

where, from Hulme (1982, equation B10),

$$\frac{E_n}{4n+1} = \int_0^1 P_1(\mu) P_{2n}(\mu) d\mu = \frac{(-1)^{n+1} (2n)!}{2^{2n+1} (n!)^2 (2n-1)(n+1)} \quad (4.23)$$

Matching with the intermediate solution gives

$$\bar{A}_{j,00} = \frac{1}{2} \epsilon^2, \quad j=1,2,\dots,N, \quad (4.24)$$

exactly, which determines the outer solution to leading order in  $\mu$ . Further details of the intermediate and inner solutions are given in the Appendix.

### 5. The mean drift force

The mean drift forces and moments on a body have been related to the far field of the first order scattering potential by Maruo (1960) and Newman (1967). The result for the mean horizontal drift force in the direction of wave advance is

$$f_x^{(2)} = \frac{\rho g A^2}{2\pi k} \left( 1 + \frac{2kh}{\sinh 2kh} \right) \int_0^{2\pi} (1 - \cos \psi) |A(\psi)|^2 d\psi \quad (5.1)$$

where  $\rho$  is here the fluid density and  $A(\psi)$  is related to the far field form of the scattered wave through

$$\phi \sim \frac{\cosh k(z-h)}{\cosh kh} A(\psi) \left( \frac{2}{\pi kr} \right)^{\frac{1}{2}} e^{ikr - i\pi/4}, \quad kr \rightarrow \infty. \quad (5.2)$$

The long-wave limit of  $f_x^{(2)}$  is zero, however the present interest is in enhancement effects which may persist for waves of large, but finite, length. The ratio of the drift force on  $N$  bodies to the drift force on an isolated body is

$$F_x^{(2)} = \frac{\int_0^{2\pi} (1 - \cos \psi) |A_N(\psi)|^2 d\psi}{\int_0^{2\pi} (1 - \cos \psi) |A_1(\psi)|^2 d\psi} \quad (5.3)$$

where  $A_N(\psi)$  gives the angular dependence of the field scattered by  $N$  bodies.

For an array of vertical cylinders the low-frequency limit of  $F_x^{(2)}$  is calculated from equations (3.12) and (3.29), after first writing equation (3.12)

in the form of equation (5.2) using the expansions of the Hankel function for large argument (Abramowitz and Stegun, 1965, p. 364). Thus

$$\lim_{\mu \rightarrow 0} F_X^{(2)} = N^2 - 2\epsilon^2 N \sum_{n=1}^N \sum_{\substack{p=1 \\ p \neq n}}^N \frac{\cos 2\alpha_{np}}{R_{np}^2} + 0(\epsilon^4) \quad (5.4)$$

This shows that the speculation that the low-frequency limit of the drift force on  $N$  cylinders is  $N^2$  times the value for an isolated cylinder is, in general, true only in the limit as  $\epsilon$  tends to zero. The existence of the  $0(\epsilon^2)$  term is consistent with the calculations for two cylinders illustrated in Figure 2 of Eatock-Taylor and Hung (1985); for two closely spaced cylinders with the line of centres perpendicular to the direction of wave advance their results show further drift force enhancement over and above an  $N^2$ -fold increase. It is interesting to note that the  $0(\epsilon^2)$  term is zero for a number of specific geometries, including two cylinders with their line of centres at an angle  $\pi/4$  to the direction of wave advance and any number ( $\geq 3$ ) of cylinders at the vertices of a regular polygon, irrespective of its orientation to the wave direction. For those cases where the term is not identically zero its sign varies with the direction of wave incidence.

The far-field form of the potential for scattering by an array of floating hemispheres is found from equations (4.13) and (4.24) using the result

$$\psi_0 \sim \left(\frac{2\pi}{Kr}\right)^{\frac{1}{2}} \exp\{-Kz + i(kr + \pi/4)\}, \quad Kr \rightarrow \infty \quad (5.5)$$

(Hulme, 1982, equation (2.8)). Hence, in this case,

$$\lim_{\mu \rightarrow 0} F_X^{(2)} = N^2, \quad (5.6)$$

exactly, and there is no higher order correction in  $\epsilon$ . The  $0(\epsilon^2)$  term for the cylinder case arises from the dipole-like terms in equation (3.12), there are no equivalent terms in the leading-order approximation to the far field for an array of hemispheres.

The dissimilarity in the far-field potentials for the two cases is a consequence of the difference in the scattering properties of the individual bodies. The vertical cylinder extends throughout the depth whereas the hemisphere is localised near the free surface in deep water. The transition from one extreme to the other may be illustrated by the solution of Miles and Gilbert (1968) for a single truncated (i.e. not extending over the full depth) cylinder



in finite depth water. Using a variational technique they derive an approximation to the far field potential of the scattered wave in the form

$$\phi(r, \psi, z) \sim \cosh K(z-h) \sum_{m=0}^{\infty} x_m H_m(kr) \cos m\psi \quad (5.7)$$

where

$$X_m \propto (G_m - J_m'(ka)) / H_m'(ka) \quad (5.8)$$

$$G_m = 2^{1/2} \frac{d}{h} \left( 1 + \frac{\sinh 2kd}{2kd} - 2\delta_{m0} \frac{\sinh^2 kd}{(kd)^2} \right) \times \sinh kh \left( 1 + \frac{\sinh 2kh}{2kh} \right)^{-3/2}, \quad (5.9)$$

and  $d$  is the clearance beneath the cylinder. Interest is in waves that are long compared to the body radius  $a$  so, if  $kh$  is taken to be  $O(1)$ , the size of  $x_m$  depends principally on the relative magnitudes of  $d/h$  and  $J_m'(ka)$ . For  $ka \ll 1$ ,

$$J_m'(ka) \sim \begin{cases} -\frac{1}{2}ka, & m = 0 \\ (\frac{1}{2}ka)^{m-1} / 2(m-1)!, & m \geq 1. \end{cases} \quad (5.10)$$

Hence, if  $d/h$  is  $O(ka)$ ,  $x_0 \sim x_1$  while  $x_m \ll x_1$  ( $m \geq 2$ ) so that to leading order in  $ka$  the far field is of the same form as equation (3.12) for cylinders extending throughout the depth. Hence it is anticipated that the drift force ratio will be given approximately by equation (5.4) for an array of truncated cylinders with little bottom clearance. On the other hand, if  $d/h = O(1)$  then  $x_0 \gg x_m$  ( $m \geq 1$ ) and the low frequency limit of the drift force ratio is well approximated by equation (5.6).

In the present work attention has been focussed on the low frequency limit of the drift force ratio. For practical purposes it is important to see how the strong interaction effects persist for shorter waves (though still long relative to body radius). The present work could, in principle, be extended to higher order for this purpose but it would be more useful to consider more realistic geometries than those considered here. Eatock-Taylor and Hung (1985) and Kagemoto and Yue (1985) have reported a small number of calculations for groups of truncated cylinders and, though they clearly illustrate the possibility of considerable drift force enhancement at non-zero frequency, more work for a greater variety of body geometries and array configurations is required.

The author is grateful to Dr. M. McIver for a number of useful comments.

Appendix; Intermediate and inner solutions

All terms in the intermediate solutions are given correct to  $O(\epsilon^4)$  while terms in the inner solutions are correct to  $O(\epsilon^4)$ .

(a) Vertical cylinders

Intermediate solution (equation (3.9)) :

$$\begin{aligned} \bar{\phi}^{(1)} = & \epsilon^2 i \sum_{n=1}^N \frac{\cos \Psi_n}{\bar{r}_n} \\ & - \epsilon^4 i \sum_{n=1}^N \sum_{\substack{p=1 \\ p \neq n}}^N \frac{\cos(\Psi_n - 2\alpha_{np})}{\bar{r}_n \bar{R}_{np}^2} \end{aligned} \quad (A1)$$

$$\bar{\phi}^{(2,1)} = \frac{1}{2} \epsilon^2 N, \quad \text{exactly.} \quad (A2)$$

$$\begin{aligned} \bar{\phi}^{(2)} = & \epsilon^2 \left\{ \frac{\pi \Gamma N}{4i} + \frac{1}{2} \sum_{n=1}^N \left( \ln \bar{r}_n - \sum_{n=1}^N \bar{\xi}_n \frac{\cos \Psi_n}{\bar{r}_n} \right) \right. \\ & + \epsilon^4 \left\{ \frac{1}{2} \sum_{n=1}^N \sum_{\substack{p=1 \\ p \neq n}}^N \frac{\cos(\Psi_n + \alpha_{np})}{\bar{r}_n \bar{R}_{np}} - \frac{1}{4} \sum_{n=1}^N \frac{\cos 2\Psi_n}{\bar{r}_n^2} \right. \\ & \left. \left. + \sum_{n=1}^N \sum_{\substack{p=1 \\ p \neq n}}^N \bar{\xi}_n \frac{\cos(\Psi_n - 2\alpha_{np})}{\bar{r}_n \bar{R}_{np}^2} \right\} \right\} \end{aligned} \quad (A3)$$

**Inner solution (equation (3.18)):**

$$\begin{aligned} \tilde{\phi}_j^{(1)} = & \epsilon i \frac{\cos \Psi_j}{\tilde{r}_j} + \epsilon^2 i \sum_{\substack{n=1 \\ n \neq j}}^N \frac{\cos \alpha_{jn}}{\bar{R}_{jn}} \\ & - \epsilon^3 i \sum_{\substack{n=1 \\ n \neq j}}^N \frac{\cos(\Psi_j - 2\alpha_{jn})}{\bar{R}_{jn}^2} (\tilde{r}_j + \tilde{r}_j^{-1}). \end{aligned}$$

$$\tilde{\phi}_j^{(2,1)} = \frac{1}{2} \epsilon^2 N, \quad \text{exactly} \quad (A5)$$

$$\begin{aligned}
\tilde{\phi}_j^{(2)} = & - \epsilon \bar{\xi} \frac{\cos \psi_j}{\tilde{r}_j} + \frac{1}{2} \epsilon^2 \ell n \epsilon \\
& + \epsilon^2 \left\{ \frac{\pi \Gamma N}{4i} + \frac{1}{2} \ell n \tilde{r}_j - \frac{1}{4} \frac{\cos 2\psi_j}{\tilde{r}_j^2} \right. \\
& \left. + \sum_{\substack{n=1 \\ n \neq j}}^N \left[ \frac{1}{2} \ell n \bar{R}_{jn} - \bar{\xi}_n \frac{\cos \alpha_{jn}}{\bar{R}_{jn}} \right] \right\} \\
& + \epsilon^3 \left\{ \sum_{\substack{n=1 \\ n \neq j}}^N \left[ \frac{1}{2} \frac{\cos(\psi_j - \alpha_{jn})}{\bar{R}_{jn}} + \bar{\xi}_n \frac{\cos(\psi_j - 2\alpha_{jn})}{\bar{R}_{jn}^2} \right] (\tilde{r}_j + \tilde{r}_j^{-1}) \right\}
\end{aligned} \tag{A6}$$

(b) Hemispheres

Intermediate solution (equation (4.8)):

$$\begin{aligned}
\bar{\phi}^{(1)} = & \frac{1}{2} \epsilon^2 \sum_{j=1}^N \frac{1}{p_j} - \epsilon^3 \frac{i}{2} \sum_{j=1}^N \frac{\sin \theta_j \cos \psi_j}{\rho_j^2} \\
& - \frac{5}{24} \epsilon^4 \sum_{j=1}^N \frac{p_2(\cos \theta_j)}{\rho_j^3}
\end{aligned} \tag{A7}$$

Inner solution (equation (4.17)):

$$\begin{aligned}
\tilde{\phi}_j^{(1)} = & \epsilon \left\{ i \frac{\sin \theta_j \cos \psi_j}{2 \tilde{\rho}_j^2} - \sum_{n=0}^{\infty} \frac{E_n p_{2n}(\cos \theta_j)}{(2n+1) \tilde{\rho}_j^{2n+1}} \right\} \\
& + \frac{1}{2} \epsilon^2 \sum_{\substack{n=1 \\ n \neq j}}^N \frac{1}{\bar{R}_{jn}} + \epsilon^3 \left\{ \sum_{\substack{n=1 \\ n \neq j}}^N \left[ \frac{i}{2} \frac{\cos \alpha_{jn}}{\bar{R}_{jn}^2} \right. \right. \\
& \left. \left. - \frac{1}{2} \frac{\cos(\psi_j - \alpha_{jn})}{\bar{R}_{jn}^2} \left( \tilde{\rho}_j + \frac{1}{2\tilde{\rho}_j^2} \right) \sin \theta_j \right] \right\} .
\end{aligned} \tag{A8}$$

## References

- Abramowitz, M. & Stegun, I.A. 1965 Handbook of Mathematical Functions. Dover, New York.
- Balsa, T.F. 1977 Potential flow interactions in an array of cylinders in array of cylinders in cross-flow. *J. Sound and Vibration*, 50, 285-303.
- Balsa, T.F. 1982 Low frequency two dimensional flows through a sparse array of bodies. *J. Sound and Vibration*, 82, 489-504.
- Balsa, T.F. 1983 Low frequency flows through an array of airfoils. *J. Sound and Vibration*, 86, 353-367.
- Eatock-Taylor, R. & Hung, S.M, 1985 Wave drift enhancement effects in multi-column structures. *Applied Ocean Research*, 7, 128-137.
- Hulme, A. 1982 The wave forces acting on a floating hemisphere undergoing forced periodic oscillations. *J. Fluid Mechanics*, 121. 443-463.
- Kagemoto, H. & Yue, D.K.P. 1986 Interactions among multiple three-dimensional bodies in water waves: an exact algebraic method. *J. Fluid Mechanics*, 166, 189-209.
- Maruo, H. 1960 The drift of a body floating in waves. *J. Ship Research*, 4 1-10.
- Miles, J.W. & Gilbert, J.F. 1968 Scattering of gravity waves by a circular dock. *J. Fluid Mechanics*, 34, 783-793.
- Newman, J.N. 1967 The drift force and moment on ships in waves. *J. Ship Research*, 11, 51-60.
- Newman, J.N. 1974 Second-order, slowly varying forces on vessels in irregular waves. *Proc. International Symposium on the Dynamics of Marine Vehicles and Structures in Waves*, University College, London, 182-186.
- Pinkster, J.A. 1979 Mean and low frequency drifting forces on floating structures. *Ocean Engineering*, 6, 593-615.
- Thorne, R.C. 1953 Multipole expansions in the theory of surface waves. *Proc. Cambridge Philosophical Society*, 49, 707-716.
- Van Dyke, M. 1975 Perturbation methods in fluid mechanics. Stanford, Parabolic Press.

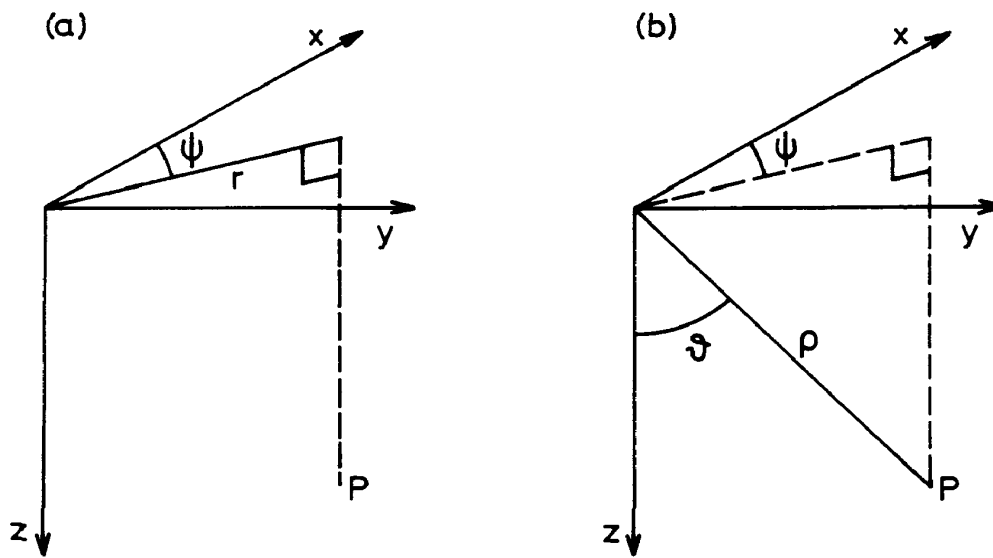


Figure 1: Definition of (a) cylindrical polar coordinates  $(r, \psi, z)$  and (b) spherical polar coordinates  $(\rho, \theta, \psi)$  of the field point P.

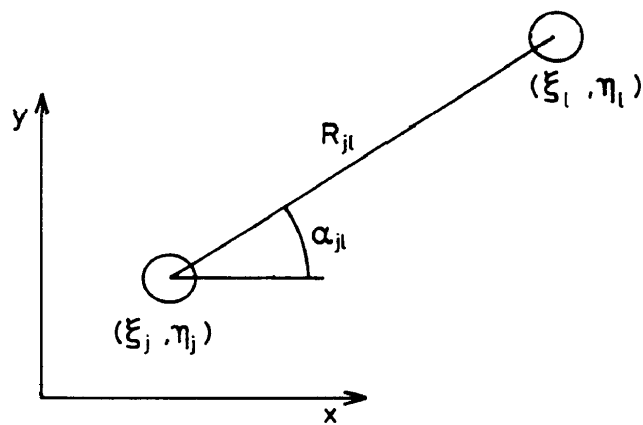


Figure 2 : Plan view of array showing bodies  $j$  and  $l$  .

**2 WEEK LOAN**

~~XB 2269522 2~~

